8. G. B. Afanas'eva, Khim. Geterotsikl. Soedin., No. 3, 324 (1970).
9. K.I. Pashkevich, G. B. Afanas'eva, and I. Ya. Postovskii, Khim. Geterotsikl. Soedin., No. 6, 746 (1971).
10. O. Fisher and E. Hepp, Berichte, 36, 1803 (1903).

CONFORMATIONAL MAPS OF MEDIUM-SIZED RINGS

É. L. Kupche and É. Lukevits

UDC 541.63

A graphical method of quantitative conformational analysis of medium-sized rings that unites earlier concepts is proposed. This method was used to obtain conformational maps of 6-8-membered rings that make it possible to unequivocally determine the conformations of real rings and to show all possible pathways of conformational transitions without depiction of the individual conformations. This approach made it possible to ascertain previously unknown conformations and pathways of conformational transitions.

In the investigation of the conformational properties of cyclic molecules one must know, first, the most probable ring conformations and, second, the possible pathways of conformational transitions. Appreciable progress has been made in the description of the conformations of medium-sized rings. At the same time, the reflection of the possible conformational transitions is almost always fraught with certain difficulties.

A general method for the qualitative description of the symmetrical conformations of medium-sized rings was proposed in the sixties by Hendrickson [1, 2]. Within the framework of this approach any symmetrical conformation can be characterized completely by a symbol that contains a horizontal line that represents a symmetry element (an axis or plane) and a set of signs of the intracyclic dihedral angles (+, 0, and −) that surround this line in the sequence that exists in the real ring.

Real molecules are usually distorted to a greater or lesser extent relative to ideal — symmetrical — conformations. For the quantitative description of these distortions in the case of five-membered rings (subsequently indicated as 5-rings) Kilpatrick developed the concept of folding coordinates (FC) 40 years ago [3]. A similar approach was subsequently used also for 6-rings [4, 5], and Cremer and Pople generalized this method for N-rings in 1975 [6]. The introduction of FC makes it possible to decrease the number of parameters necessary for the description of the form of the ring to N − 3.

Despite all of the advantages of FC, this method has not yet been widely used. In most studies the authors, as before, use the signs of the dihedral angles or simply projections of the rings to determine the conformations of medium-sized rings. This often leads to various misunderstandings. In our opinion, one of the reasons for this is the lack of visual descriptiveness when FC are used. As a result of this, the concept of FC is extremely abstract.

In this paper we present conformational maps of medium-sized (N = 6-8) rings that make it possible to solve, in part, the problems mentioned above.

Folding Coordinates

According to Cremer and Pople [6], for any N-ring one can select a plane in such a way that the deviations of the atoms from it (z_j) satisfy the equation (1)

$$z_j = (2/N)^{1/2} \sum_{m=2}^{M} q_m \cos\left[\psi_m + 2\pi m(j-1)/N\right] + \delta_{N,2(M+1)}(-1)^{j-1}N^{-1/2}q_{N/2}, \quad (1)$$

where N = (N − 1)/2 if N is odd or M = (N/2) − 1 if N is even, j = 1, 2, ..., N. q_m are the folding amplitudes, ψ_m are the phase angles that describe the various forms of folding, δ = 1 if N is even, and δ = 0 if N is odd. One can calculate N − 3 folding coordinates using

Institute of Organic Synthesis, Academy of Sciences of the Latvian SSR, Riga 226006.
Translated from Khimiya Geterotsiklicheskikh Soedinenii, No. 4, pp. 542-559, April, 1988. Original article submitted July 7, 1986; revision submitted October 5, 1987.

0009-3122/88/2404-0449$12.50

deviations z_j from Eqs. (2)-(4):

$$q_m \cos \psi_m = (2/N)^{1/2} \sum_{j=1}^{N} z_j \cos [2\pi m (j-1)/N], \tag{2}$$

$$q_m \sin \psi_m = -(2/N)^{1/2} \sum_{j=1}^{N} z_j \sin [2\pi m (j-1)/N], \tag{3}$$

$$q_{N/2} = (1/N)^{1/2} \sum_{j=1}^{N} z_j \cos [\pi (j-1)], \tag{4}$$

$$Q^2 = \sum_{m=2}^{M} q_m^2 + \delta_{N,2(M+1)} \cdot q_{N/2}^2. \tag{5}$$

The additional parameter $q_{N/2}$ is calculated in the case of even-numbered rings; Q is the total folding amplitude (5).

However, it was subsequently found that this method describes the form of the rings poorly in the case of different bond lengths. Zefirov and Palyulin [7] attempted to eliminate this inadequacy by using the sin $(\varphi_j/2)$ values instead of deviations z_j, where φ_j are the intracyclic dihedral angles. They obtained the following equations:

$$q_m \cos \psi_m = (2/N)^{1/2} \sum_{j=1}^{N} \sin (\varphi_j/2) \cos [2\pi m (j-1)/N], \tag{6}$$

$$q_m \sin \psi_m = -(2/N)^{1/2} \sum_{j=1}^{N} \sin (\varphi_j/2) \sin [2\pi m (j-1)/N], \tag{7}$$

$$q_{N/2} = (1/N)^{1/2} \sum_{j=1}^{N} \sin (\varphi_j/2) \cos [\pi (j-1)], \tag{8}$$

$$Q^2 = \sum_{m=2}^{M} q_m^2 + q_{N/2}^2 \cdot \delta_{N,2(M+1)}. \tag{9}$$

Torsion angles φ_j can be regenerated from the FC by means of Eq. (10):

$$\varphi_j = 2 \arcsin \left\{ (2/N)^{1/2} \sum_{m=2}^{M} q_m \cos [\psi_m + 2\pi m (j-1)/N] + (1/N)^{1/2} \delta_{N,2(M+1)} q_{N/2} \cos [\pi (j-1)] \right\}. \tag{10}$$

The derivation of the relationships between z_j and φ_j presented subsequently [8] shows that Eqs. (6)-(10) are approximate. The Fourier transformation model proposed by Cano and coworkers [9, 10] is also approximate, since in this case the zero and first terms, because of their insignificant contribution, are not taken into account to obtain the minimum number of parameters (N − 3). In this model the folding parameters are calculated from the equations

$$q_m \cos \psi_m = (2/N) \sum_{j=1}^{N} \varphi_j \cos [2\pi m (j-1)/N], \tag{11}$$

$$q_m \sin \psi_m = -(2/N) \sum_{j=1}^{N} \varphi_j \sin [2\pi m (j-1)/N], \tag{12}$$

$$q_{N/2}=(1/N)\sum_{j=1}^{N}\varphi_j\cos[\pi(j-1)], \tag{13}$$

where q_m has the dimensions of an angle.

Dihedral angles φ_j can be regenerated from the equation

$$\varphi_j=\sum_{m=2}^{M}q_m\cos[\psi_m+2\pi m(j-1)/N]+\delta_{N,2(M+1)}q_{N/2}\cos[\pi(j-1)]. \tag{14}$$

Despite the approximate character of Eqs. (6)-(10) and (11)-(13), the use of dihedral angles for calculating the FC has a number of advantages. Thus, in contrast to coordinates z_j, which can be obtained primarily by diffraction methods, the dihedral angles, in principle, can be determined by the NMR method in solutions.

The use of dihedral angles makes it possible to decrease the number of starting data to N − 2 [11], and the FC themselves calculated in this way are less sensitive to differences in the bond lengths in the ring [7].

Construction of Conformational Maps

In the general case any point in the space of the FC is a certain conformation of the ring. Consequently, the number of possible conformations is, in principle, unlimited. In addition, on the basis of the signs of the dihedral angles and the symmetry elements of the N-ring one can construct a certain system of reference standard conformations, with respect to which the geometries of real molecules can be conveniently analyzed.

The folding coordinates by means of Eqs. (15) and (16)

$$\operatorname{tg}\Theta_m=q_M/q_m \quad \text{(for odd N)} \tag{15}$$

$$\operatorname{tg}\Theta_m=q_{N/2}/q_m \quad \text{(for even N)} \tag{16}$$

can be represented in a polar system of coordinates ($\{\Theta_m\}$, $\{\psi_m\}$, Q)* selected in such a way that $-\pi/2 < \Theta_m < \pi/2$. This makes it possible to separate the parameters that characterize the conformation of the ring (Θ_m, ψ_m) and the degree of its folding (Q).

It is known that for constant Q the conformations of N-rings form the surface of an (N − 3)-dimensional sphere [6]. In the case of 6-rings this is the ordinary three-dimensional sphere, the radius Q of which is a measure of the degree of folding of the ring (Fig. 1) [1]. The completely planar ring is found at the center of the sphere. For the construction of the maps of the surfaces of such spheres we used the Hendrickson assumption that a change in the conformation of the ring occurs with a change in the signs of the dihedral angles. Consequently, the most important sections of the conformational maps are the points where the dihedral angle changes its sign, i.e., where $\varphi_j = 0$. In the general case these points can be found from Eqs. (10) or (14) under the conditions that $\varphi_j = 0$. Using polar coordinates, for odd-numbered rings in both cases we obtain Eq. (17):

$$\sum_{m=2}^{M-1}\operatorname{ctg}\Theta_m\cos[\psi_m+2\pi m(j-1)/N]=-\cos[\psi_M+2\pi M(j-1)/N]. \tag{17}$$

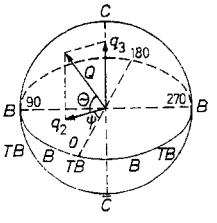

Fig. 1. Spherical representation of the conformational space of 6-rings. See Fig. 3 for the designations of the conformations.

*For conversion to the polar system of coordinates that is customary in mathematics ($0 < \Theta_m < \pi$) tg in Eqs. (15) and (16) should be replaced by ctg. The frame of reference that we selected seems more convenient in this case, since it simplifies the interrelationship between the FC of enantiomeric and invertomeric conformations and also reflects more graphically the symmetry properties of the conformational maps.

For even-numbered rings we obtain the equation

$$C\sum_{m=2}^{M}\operatorname{ctg}\Theta_m\cos\left[\psi_m+2\pi m(j-1)/N\right]=-\cos\left[\pi(j-1)\right], \tag{18}$$

where constant C depends on the method used to calculate the FC.

In the case of the Zefirov–Palyulin method (10) $C=\sqrt{2}$, whereas C = 1 when the approach of Cano and co-workers (14) is used. Thus for the transition from the FC of Zefirov and Palyulin to the FC of Cano one can use the expression

$$\operatorname{tg}\Theta_m\,(\text{ Zefirov}-\text{Palyulin})=\sqrt{2}\operatorname{tg}\Theta_m\ \ (\text{Cano}) \tag{19}$$

We will subsequently use Zefirov–Palyulin method (6)-(10), since it more accurately reproduces the starting data vis-a-vis the minimal set of parameters.

The symmetry elements are no less important parameters that characterize the conformation of the ring. In the study of the three-dimensional structures of cyclic molecules and in the investigation of dynamic processes in solutions the conformations that have symmetry elements (the symmetrical conformations) are customarily regarded as the standard conformations. We therefore used the symmetry elements as an additional criterion that characterizes the conformation of the ring.

6-Membered Rings

For 6-rings the conformational map can be obtained from the equation

$$\operatorname{tg}\Theta=-\sqrt{2}\cos\left[\psi+2\pi(j-1)/3\right]/\cos\left[\pi(j-1)\right], \tag{20}$$

which is a special case of Eq. (18) for N = 6 and $C=\sqrt{2}$.

The graphical depiction of the solution of this equation (Fig. 2) makes it possible to divide the surface of the three-dimensional sphere shown in Fig. 1 into a number of regions, each of which corresponds to a set of related conformations. The points where the sign of the dihedral angle changes ($\varphi_j = 0$) form lines of the sinusoidal type. Conformations for which one of the dihedral angles is equal to zero ("monoplanar" conformations [12]) are found on these lines (subsequently designated as 0-lines). Biplanar conformations are found at the points where two 0-lines intersect. Nonplanar conformations are found in the fields between the 0-lines. Thus this map reflects all of the theoretically possible conformations and conformational transitions for 6-rings. A completely planar ring ($\varphi_j = 0$ for all j) in this case is not regarded as an independent conformation, since this case is realized for any conformation when $Q \to 0$, i.e., at the center of the sphere. However, φ_j have finite values other than zero even for benzene derivatives (for example, see XI in Table 2).

As demonstrated in [1], the chair (C) conformation and its invertomer ($\bar{C}$) are found at the poles of the sphere ($\Theta = 90°$). The B and TB conformations are situated on the equator ($\Theta = 0°$). The remaining conformations are situated between the equator and the poles. The symmetrical conformations (Fig. 3) are found at $\psi = n\pi/6$ (n = 1, 2, ..., 12), forming unique meridians on the surface of the sphere. In the case of even n values the conformations have a symmetry plane (C_s), while in the case of odd n values they have a second-order symmetry axis (C_2).

It is apparent from Fig. 2 that for 6-rings one can isolate eight types of standard symmetrical conformations, which are presented in Fig. 3 — one monoplanar, three diplanar, and four nonplanar conformations. The coordinates of these conformations are presented in Table 1. Some difficulties arise in determining the coordinates of the nonpolanar standard symmetrical conformations. In analyzing the conformations of 7-rings Cano and co-workers [9, 10] used the criterion of identical dihedral angles. However, this approach led the authors to the development of "phantom" conformations, i.e., those that differ only in the absolute value of the dihedral angles but have the same sequence of dihedral angles and the same symmetry elements. To avoid this we used the criterion of an identical distance (with respect to Θ) to the closest planar conformations.

For even-numbered rings the conformations that are found at the poles and on the equator (equators) have increased symmetry. For this reason in the neighborhood of the poles and the equator (equators) one can isolate families of conformations that have the same sequence of dihedral angles but differ with respect to symmetry elements. A classical example is the "crown" family for 8-rings, which consists of three "subconformations": the crown (D_{4d}), chair-chair (C_{2v}), and twisted chair-chair (D_2). For 6-rings similar "subconforma-

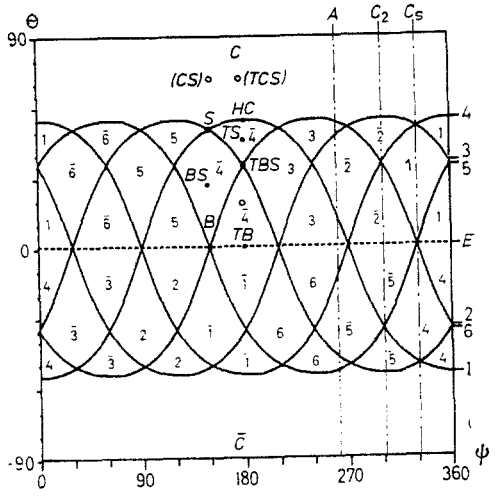

Fig. 2. Conformational map of 6-rings: the sinusoidal lines are the points where dihedral angle $\varphi_j = 0$; the ordinal number (j) of the corresponding dihedral angle is presented on the right-hand side of the map; the sites of the indicator atoms in the ring are designated by the numbers of the map; the inverted conformations are designated by the numbers with lines over them; the coordinates of the standard conformations, noted on the map by small circles, are presented in Table 1; the equator (E) and the pathways of inversion for the chair (C) conformation are shown on the map by dash lines (see the text and Fig. 5).

tions" can be isolated for the "chair" family, the chair (C) conformation, which has D_{3d} symmetry, the chair-sofa (CS) conformation with C_s symmetry, and the twisted chair-sofa (TCS) conformation with C_2 symmetry. A similar subconformation can also be detected between the TB and TBS conformations (in Fig. 2 the "subconformations" are designated by clear circles). Since the sequence of the dihedral angles in these families is retained, we did not isolate conformations of lower symmetry as independent standard conformations.

The conformations that are not found on the meridians ($\psi \neq n\pi/6$) are unsymmetrical. i.e., they are distorted relative to the symmetrical conformations. It should be noted that most real rings exist in unsymmetrical conformations. The calculation of the FC for the rings of various molecules makes it possible by means of this map to readily determine the closest symmetrical conformation as well as the character and degree of distortion of the ring.

Principles of Systematization of the Symmetrical Conformations and Examples of the Use of Conformational Maps. To establish the conformations of the individual rings of various compounds one must renumber the atoms in the ring in accordance with the IUPAC rules [13]. For this one must determine atom 1 (subsequently designated the indicator atom) and atom 2 and orient the ring in such a way that the atoms in the ring are numbered clockwise. Several examples for I-XI are presented in Table 2 (also see [6]).

With the exception of the ideal chair conformation, different positions in the ring are generally nonequivalent. The conformations therefore also differ with respect to the location of the indicator atom (usually the heteroatom or the atom that bears a substituent). The numbering of the positions for the various conformations is usually carried out relative to the atom or bond that intersects the symmetry element [1, 2]. However, this definition is ambiguous, since, first, a given symmetry element always intersects two atoms (bonds) in the ring and, second, in the case of even-numbered rings the conformations that are found on the equator have several symmetry elements. To allocate the conformations on the map one must unambiguously determine the order of numbering of the positions in the ring. For this we used the following criterion: the conformations that are found on the same meridian should have the same numbering of the positions relative to a common symmetry element — the C_s plane or the C_2 axis. In this case the order of numbering for conformations with C_2 symmetry can be selected in such a way that the twisted and corresponding untwisted conformations (the so-called pseudorotation partners [2]) are side by side on the map. The numbering of the posi-

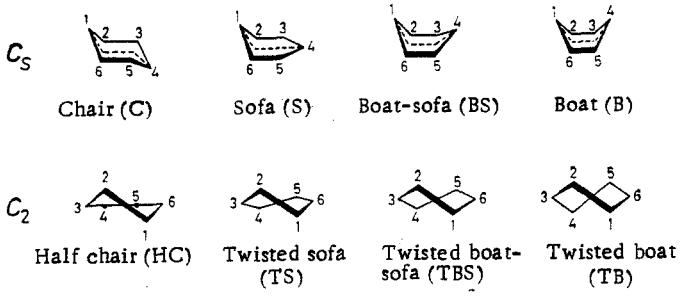

Fig. 3. Symmetrical conformations of 6-rings.

TABLE 1. Symmetrical Conformations of a 6-Ring Situated on the Surface of a Three-dimensional Sphere with Radius Q = 0.8

Folding coordinates		Dihedral angles φ^0						Conformation*	Hendrickson symbol	Symmetry group
ψ°	Θ°	φ_1	φ_2	φ_3	φ_4	φ_5	φ_6			
—	90	38	−38	38	−38	38	−38	*C*	$\frac{+-+}{-+-}$	D_{3d}
330	51	61	−29	0	0	29	−61	*S*-1	$\frac{+-0}{-+0}$	C_s
330	25	60	−16	−26	26	16	−60	*BS*-1	$\frac{+--}{-++}$	C_s
330	0	47	0	−47	47	0	−47	*B*-1 (4)	$\frac{+0-}{-0+}$	C_{2v}
360	55	64	−47	15	0	15	−47	*HC*-1	$+\frac{-+}{-+}0$	C_2
360	45	68	−46	8	11	8	−46	*TS*-1	$+\frac{-+}{-+}+$	C_2
360	35	69	−44	0	22	0	−44	*TBS*-1	$+\frac{-0}{-0}+$	C_2
360	0	55	−27	−27	55	−27	−27	*TB*-1 (4)	$+\frac{--}{--}+$	D_2

*Equivalent conformations are indicated in parentheses. Thus the B-1 and B-4 conformations are equivalent.

tions of the symmetrical conformations of 6-rings taking these criteria into account is shown in Fig. 3. The numbers on the conformational map (Fig. 2) reflect the position occupied by the indicator atom in the given conformation. The invertomers are designated by lines over the numbers. The invertomers are conformations (for example, S-5 and S-$\bar{5}$) that have dihedral angles that are identical in absolute values but have opposite signs.

S-5 $\frac{+-0}{-+0}$ S-$\bar{5}$ $\frac{-+0}{+-0}$

As an example we calculated the FC and determined the conformations of the 6-rings of I-XI (Table 2); the location of these compounds on the conformational map of 6-rings are shown in Fig. 4.

Pathways of Conformational Transitions. The conformational map presented in Fig. 2 reflects the interrelationship between all conformations of the 6-rings. This makes it possible to detect all possible pathways of conformational transitions without resorting to figures of the individual conformations.

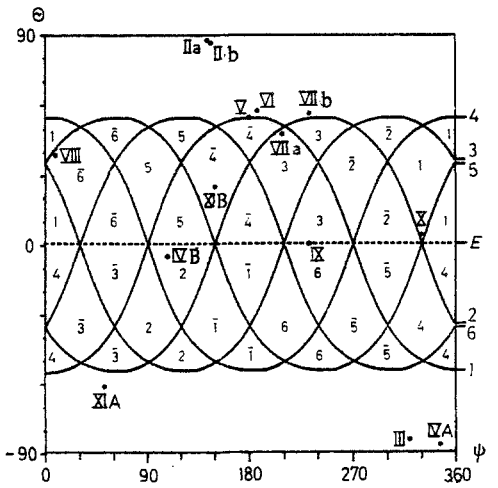

Fig. 4. Locations of the 6-rings of I-XI on the conformational map.

TABLE 2. Dihedral Angles and Folding Coordinates of the 6-Rings of I–XI

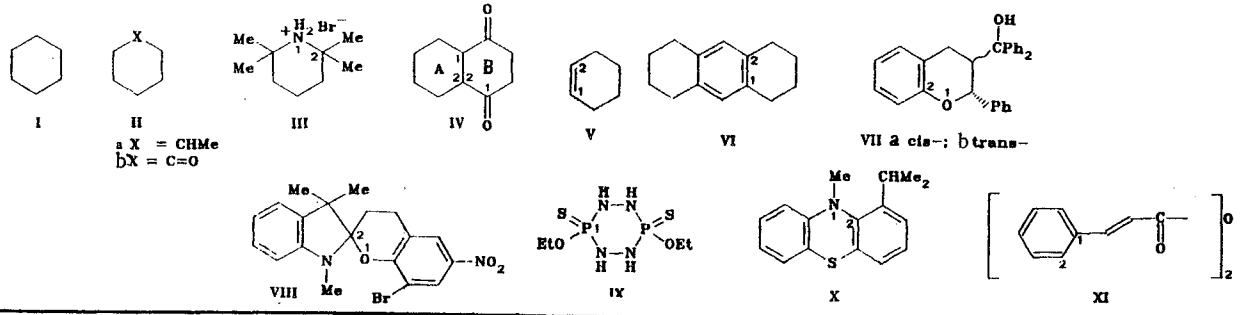

Compound	Dihedral angles φ^0						Folding coordinates			Assignment of the conformation*	Lit.
	φ_1	φ_2	φ_3	φ_4	φ_5	φ_6	θ°	ψ°	Q		
I	56,0	−56,0	56,0	−56,0	56,0	−56,0	90,0	—	1,15	*C*	[12]
IIa	53,0	−55,0	56,0	−56,0	55,0	−53,0	88,8	150,0	1,12	*C* (*S*-$\bar{4}$, 3%)	[14]
IIb	53,0	−54,0	56,5	−56,5	54,0	−53,0	88,6	150,0	1,12	*C* (*S*-$\bar{4}$, 3%)	[15]
III	−50,0	51,7	−59,3	59,2	−51,2	49,5	−86,2	327,2	1,10	$\bar{C}$ (*S*-4, 10%)	[16]
IVA**	−52,4	54,1	−56,2	56,9	−55,4	53,1	−88,4	346,9	1,12	$\bar{C}$ (*HC*-4, 4%)	[17]
IVB	−20,3	−28,9	47,0	−13,9	−35,3	52,2	−4,7	110,0	0,74	*TB*-2 (*B*-2, 33%; *TBS*-2, 13%)	[17]
V	0,0	−15,0	45,0	−60,0	45,0	−15,0	55,1	180,0	0,76	*HC*-$\bar{4}$	[18]
VI	3,8	−18,0	47,5	−64,2	49,2	−19,6	58,4	181,8	0,82	*HC*-$\bar{4}$ (*C*, 10%)	[19]
VIIa	−3,8	2,4	26,0	−53,0	54,0	−25,0	48,1	209,5	0,71	*S*-3 (*B*-3, 5%)	[20]
VIIb	10,0	−2,4	22,0	−46,0	55,0	−37,0	57,0	226,8	0,71	*HC*-3 (*S*-3, 47%)	[20]
VIII	26,6	−19,4	3,6	7,8	−0,6	−17,9	38,9	5,5	0,33	*TBS*-1 (*S*-$\bar{6}$, 18%)	[21]
IX	−32,1	63,0	−28,7	−32,1	63,0	−28,7	0,0	232,2	0,91	*TB*-3 (*B*-3, 6%)	[22]
X	38,1	0,7	−32,0	33,1	−2,8	−32,7	2,1	331,5	0,60	*B*-1 (*BS*-1, 8%)	[23]
XIA**	−1,4	0,4	−1,9	4,2	−5,1	3,8	−59,2	53,7	0,07	*HC*-$\bar{3}$ ($\bar{C}$, 21%)	[24]
XIB	−2,4	−1,1	4,7	−4,9	1,2	2,2	22,8	151,4	0,07	*BS*-$\bar{4}$ (*B*-$\bar{4}$, 10%)	[24]

*The mode of distortion of the principal conformation and the degree of this distortion are indicated in parentheses. Thus in IIa and IIb the ring has the C conformation with 3% distortion towards S-$\bar{4}$.

**Two different rings.

The inversion of cyclohexane is a classical example of conformational transitions for 6-rings. The two invertomers of the principal conformation of cyclohexane C and $\bar{C}$ are found at opposite poles of the globe. Consequently, ring inversion in this case can simply (disregarding a change in Q) be regarded as migration of a point from one pole to the other along the surface of the sphere. Three possible mechanisms of the inversion of cyclohexane — with retention of the symmetry plane (C_s), with retention of the symmetry axis (C_2), and an asymmetric mechanism (A) — are usually discussed. In addition to figures of the individual conformations, it has been proposed [12] that special schemes, as an example of which the scheme of the inversion of cyclohexane presented here (Fig. 5) may serve, be used to reflect the various inversion mechanisms, whereas conformational maps (Fig. 2) make it possible to show all mechanisms of conformational interchange in greater detail and without depiction of the individual conformations. On such maps one can detect all of the transition conformations and torsion angles that take on zero values in this process.

It is also apparent from Fig. 2 that, in contrast to the C_s and C_2 mechanisms, the asymmetric pathway can be selected more arbitrarily. It should be noted that the pathways of conformational transitions evidently form more complex trajectories for real molecules.

In the general case the ring inversion process for any conformation can be represented as migration to a diametrically opposed point of the sphere; in the case of nonplanar conformations six different 0-lines must intersect, which corresponds to inversion of the signs for all of the dihedral angles. The inversion process leads to complete axial-equatorial interchange of the substituents in the ring. (Averaging of the chemical shifts and the spin-spin coupling constants is observed in the NMR spectra in this case.)

Pseudorotation can simply be represented as migration of a point along a parallel, i.e., a change in ψ vis-à-vis relatively small changes in Θ. The complete pseudorotation cycle leads to the starting conformation. In the process of pseudorotation axial-equatorial interchange of the substituents occurs only partially. Pseudorotation in the B—TB family is an exception. It is apparent from Fig. 2 that, in principle, pseudorotation may take place through various transition conformations. Thus the symmetrical HC, TS, or TB conformations may act as pseudorotation partners for the S conformation.

Energy Considerations. In real molecules conformational transitions are realized along more or less complex trajectories. To establish these trajectories one must calculate the energy surface of the sphere (the conformational energy map),* as was done, for example. for cyclohexane and 1,3-dioxane [25]. However, this surface will differ for different molecules. Moreover, a conformation that is a transition state for some molecules may prove to be a ground state for others. However, the conformational maps presented in our paper are universal in the sense that they make it possible to investigate all possible pathways of conformational transitions for any molecules simply and graphically.

To a first approximation, the most probable pathways of conformational transitions can be established by taking into account, for example, the barriers to rotation about the individual bonds, the orientation of the bulky substituents, etc. For example, for compounds that contain a double bond the 0-line corresponding to this bond can, to a first approximation, be regarded as the most probable pathway of conformational transitions, since rotation about a double bond has a high energy. In Fig. 2 one can easily detect all of the transition conformations that are usually considered for inversion of the HC conformation of cyclohexene derivatives [12]. This map can be used in the statistical treatment of data on the conformations of various series of compounds and to predict the most probable pathways of conformational transitions.

7-Membered Rings

The conformational map of 7-rings can be obtained from the equation

$$\operatorname{tg}\Theta = -\cos\left[\psi_2 + 4\pi(j-1)/7\right]/\cos\left[\psi_3 + 6\pi(j-1)/7\right], \quad (21)$$

which is a special case of Eq. (17) for N = 7.

In this case all conformations of the 7-rings form the surface of a four-dimensional sphere. The complete conformational map of this sphere is three-dimensional.

*Strictly speaking, the radius of the sphere Q also changes in the process of conformational transitions; however, for greater clarity in the conformational energy maps the changes in Q are usually not reflected.

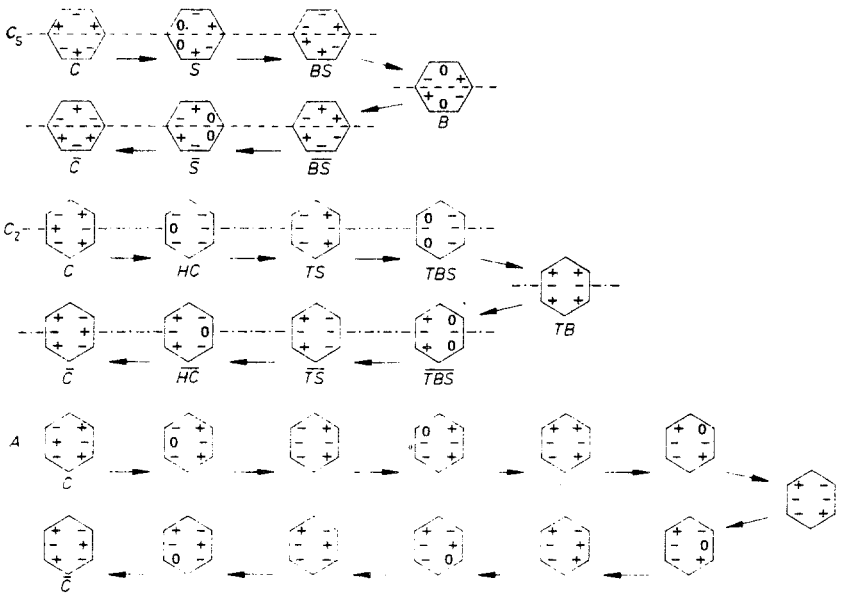

Fig. 5. Scheme of the classical mechanisms of inversion of the 6-ring for the C conformation of cyclohexane [12]: C_s) with retention of the symmetry plane; C_2) with retention of the symmetry axis; A) asymmetric mechanism.

The points where the dihedral angle changes its sign form O-surfaces, one of which is shown in Fig. 6. The complete map of 7-rings is the superimposition of seven O-surfaces. The depiction and analysis of this map are complex and difficult to represent graphically. It is more convenient to use sections of this map, selecting one of the parameters as being constant. An alternative and more universal method of constructing the map is the use of a pseudorotation pathway as one coordinate, since all symmetrical conformations of 7-rings are located on the pseudorotation coordinate.

There are two pseudorotation coordinates — $\psi_2 = 3\psi_3$ and $\psi_2 = 3\psi_3 + 180°$ — for 7-rings [8, 9]. This is associated with the fact that in the calculation of the FC the ψ_m values depend on the choice of the sign of q_m. The existence of two pseudorotation coordinates is a consequence of the fact that q_m is always chosen as positive. In the corresponding selection of the sign of q_m one can use only one pseudorotation coordinate. For this one must take into account the fact that inversion of the sign of Θ is equivalent to a 180° change in ψ_2 (or ψ_3).

The conformational map of 7-rings — the cross section with respect to pseudorotation coordinates $\psi_2 = 3\psi_3$ — is shown in Fig. 7. The symmetrical conformations are located at $\psi_3 = n\pi/14$. In the case of even N the conformations have a symmetry plane (C_s), while in the case of odd n they have a second-order symmetry axis (C_2). This map is considerably more complex than the map of 6-rings; this is associated with the increase in the number of possible conformations and conformational transitions.

The conformational map of 7-rings does not have poles, since the two components q_2 and q_3 are associated with pseudorotation phase angles ψ_2 and ψ_3, respectively. For this reason, it is more convenient to place this map on the surface of a torus (Fig. 8)*; on the external

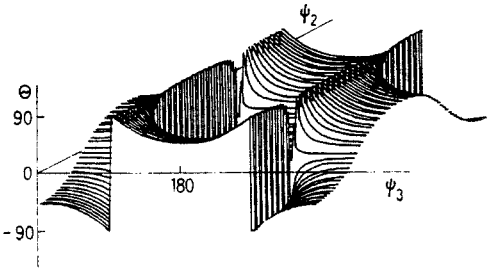

Fig. 6. O-Surface of the conformational map of 7-rings when j = 1.

*The surface of a torus was previously used to plot the pseudorotation pathway of individual conformations of 7-rings [26].

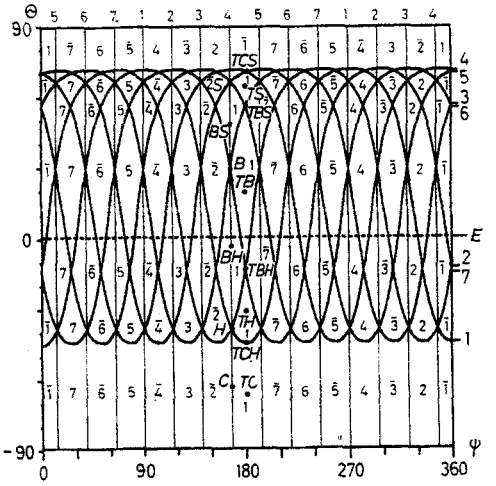

Fig. 7

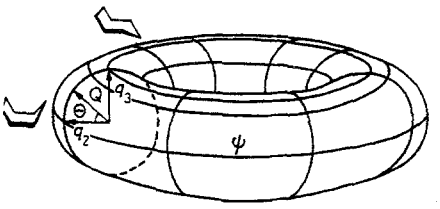

Fig. 8

Fig. 7. Cross section of the conformational map of 7-rings with respect to the pseudorotation coordinate ($\psi_2 = 3\psi$ and $\psi = \psi_3$). The equator (E) is designated by the dash line.

Fig. 8. Toroidal representation of the conformational space of 7-rings.

equator the pseudorotation coordinate is such that $\psi_2 = 3\psi_3$, while $\psi_2 = 3\psi_3 + 180°$ on the internal equator.

The total number of symmetrical conformations for 7-rings is 14 — four nonplanar, four monoplanar, three biplanar, and three triplanar.* The FC of the standard symmetrical conformations are presented in Table 3. The criteria of their selection are similar to those described for 6-rings. The numbering of the positions for various conformations is shown in Fig. 9.

A substantial difference between the map of 7-rings and the map for 6-rings (an even-numbered rings in general) is the fact that it is unsymmetrical relative to the equator. The conformations on the equator and at the poles (in the toroidal representation) do not have additional symmetry. Because of this, there is no reason to isolate individual conformations on the equator and at the poles.

Just as in the case of 6-rings, one can isolate three types of conformational transitions. a) Transitions with retention of the symmetry plane (C_S). The pathway of this mechanism on the map coincides with the vertical O-lines. Thus the inversion of the C conformation, according to this mechanism, occurs through triplanar conformations S, B, and H. b) Transitions with retention of the symmetry axis (C_2). For example, the inversion of the TC conformation, according to this mechanism, occurs through biplanar conformations TSC, TBS, and TBH. c) Asymmetrical transitions occur at intermediate ψ_2 and ψ_3 values, which may also differ from the pseudorotation coordinate.

In addition to these mechanisms, inversion in 7-rings may also be realized via pseudorotation; in the case, as one can see from the map, for the TC conformation this occurs as a result of the intersection of seven O-lines. For the TS conformation the O-lines must intersect 21 times in this pathway, since the intersection of each O-line occurs three times.

In the case of markedly distorted rings ψ_2 and ψ_3 may differ markedly from the pseudorotation coordinate. In this case the use of this map is generally inaccurate. However, the use of this map is permissible near the equator ($q_3 \to 0$) or poles ($q_2 \to 0$) where the contribution of one of the q_m parameters is not substantial. In the remaining cases one must construct special maps, selecting one of the parameters (Θ, for example) as constant. The program for the construction of such maps is available for interested individuals.

*At the points with coordinates $\Theta = 72°$, $\psi_2 = 3\psi_3$, and $\psi_3 = n\pi/14$ for odd n the O-lines with identical j intersect. For this reason, the apparent biplanar conformations at the given points do not actually exist.

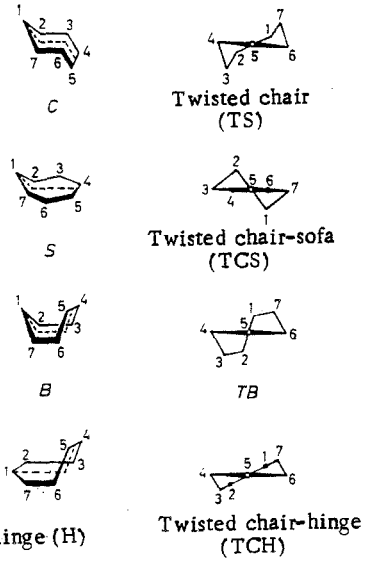

Fig. 9. Some symmetrical conformations of 7-rings.

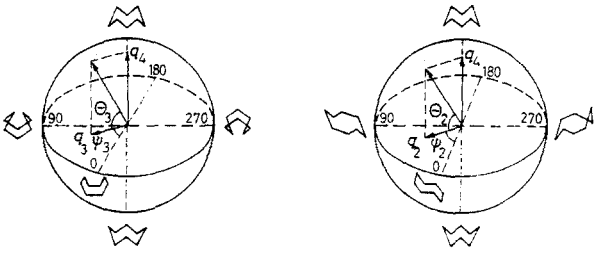

Fig. 10. Presentation of the conformation of 8-rings in a system of polar coordinates.

8-Membered Rings. The form of 8-rings is described by four polar coordinates Θ_2, Θ_3, ψ_2, and ψ_3 and the degree of folding Q. The conformational map of 8-rings can be obtained by solution of Eq. (22), which is a special case of Eq. (18) for N = 8 and C = $\sqrt{2}$:

$$\cos[\psi_2+\pi(j-1)/2]/\operatorname{tg}\Theta_2+\cos[\psi_3+3\pi(j-1)/4]/\operatorname{tg}\Theta_3=-\cos[\pi(j-1)]/\sqrt{2}. \quad (22)$$

All conformations of 8-rings form the surface of a five-dimensional sphere, while the complete conformational map of this sphere is four-dimensional.* This circumstance significantly complicates the depiction of this map. Certain simplifications must therefore be used.

The conformations for which one of the parameters $q_m = 0$ (m = 2, 3), i.e., $\Theta_m = 90°$, can be placed on the surface of a three-dimensional sphere. Thus the complete conformation space of 8-rings can be represented by the interaction of two three-dimensional spheres Θ_2, ψ_2 and Θ_3, ψ_3 (Fig. 10), and any conformation of 8-rings can be represented by the coordinates of the point of contact of these spheres. Conformational maps of these spheres are shown in Figs. 11 and 12. The latter resemble the conformational map of 6-rings. The symmetrical conformations are located at $\psi_2 = n\pi/4$ and $\psi_3 = n\pi/8$. The conformations on the Θ_2, ψ_2 sphere have higher symmetry as compared with the corresponding conformations on the Θ_3, ψ_3 sphere. The conformations at the poles and on the equators have increased symmetry. On the basis of the symmetry criterion one can therefore isolate the corresponding "subconformations." The chair-chair (CC) and twisted chair-chair (TCC) conformations, which differ from the "crown" conformation only with respect to the smaller number of symmetry elements, are a classical example of this. The FC of the highly symmetrical conformations of 8-rings are pre-

*The conformation space of 8-rings on the basis of the FC was previously discussed in [27].

TABLE 3. Symmetrical Conformations of 7-Rings Situated on the Surface of a Four-Dimensional Sphere with Radius Q = 1.0

Folding coordinates			Dihedral angles φ^0							Conformation
$\psi_2°$	$\psi_3°$	$\Theta°$	φ_1	φ_2	φ_3	φ_4	φ_5	φ_6	φ_7	
141,45	167,15	−76,4	48,1	−54,9	40,8	0	−40,8	54,9	−48,1	*C*-1
141,45	167,15	−38,7	0	−52,5	67,0	0	−67,0	52,5	0	*H*-1
141,45	167,15	−4,8	−43,8	−30,9	65,2	0	−65,2	30,9	43,8	*BH*-1
141,45	167,15	29,1	−76,4	0	40,1	0	−40,1	0	76,4	*B*-1
141,45	167,15	48,5	−83,7	18,3	19,8	0	−19,8	−18,3	83,7	*BS*-1
141,45	167,15	66,0	−80,5	33,4	0	0	0	−33,4	80,5	*S*-1
180,0	180,0	−77,3	47,6	−52,7	51,1	−21,8	−21,8	51,1	−52,7	*TC*-1
180,0	180,0	−45,0	0	−29,7	70,4	−37,3	−37,3	70,4	−29,7	*TCH*-1
180,0	180,0	−29,5	−23,3	−15,4	71,4	−40,8	−40,8	71,4	−15,4	*TH*-1
180,0	180,0	−13,9	−46,0	0	66,4	−41,2	−41,2	66,4	0	*TBH*-1
180,0	180,0	24,5	−90,2	35,9	34,9	−29,4	−29,4	34,9	35,9	*TB*-1
180,0	180,0	55,3	−96,1	55,2	0	−10,6	−10,6	0	55,2	*TBS*-1
180,0	180,0	62,8	−92,1	57,7	−8,7	−5,3	−5,3	−8,7	57,7	*TS*-1
180,0	180,0	70,4	−86,1	59,2	−17,5	0	0	−17,5	59,2	*TCS*-1

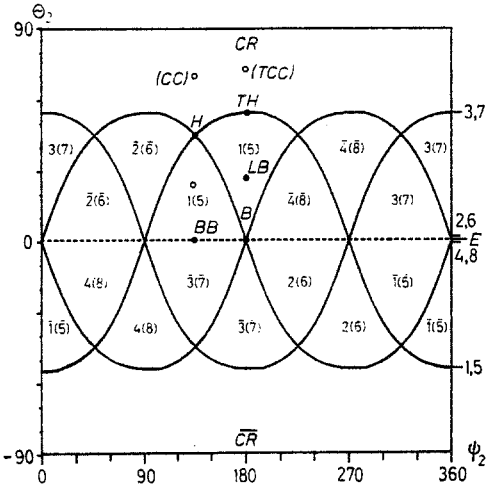

Fig. 11

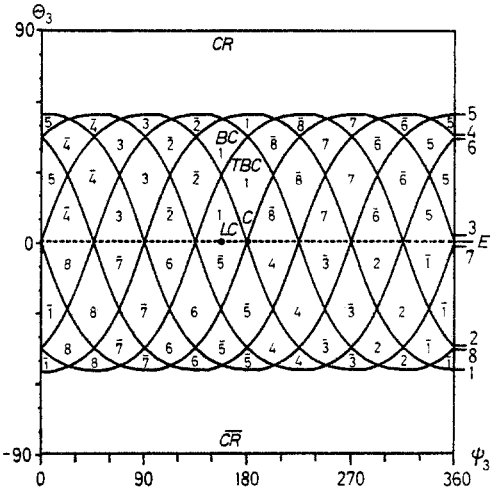

Fig. 12

Fig. 11. Conformational map of the Θ_2, ψ_2 sphere of 8-rings ($\Theta_3 = 90°$): the O-lines are dual; their ordinal numbers (j) are indicated on the right-hand side of the map; the equator (E) is designated by the dash line.

Fig. 12. Conformational map of the Θ_3, ψ_3 sphere of 8-rings ($\Theta_2 = 90°$): the ordinal numbers of the O-lines (j) are shown on the right-hand side of the map; the equator (E) is shown by the dash line; the precise FC are shown only for the highly symmetrical C and LC conformations (see the text).

sented in Table 4. The numbering of the positions for the principal conformations is shown in Fig. 13. The criteria of their selection are similar to those described for 6-rings.

Unfortunately, for real rings all of the q_m parameters usually have finite values. The sum of the conformational maps presented in Figs. 11 and 12 for such rings is therefore inaccurate to a greater or lesser extent. In this case one must construct cross-section maps in the case of two constant parameters. If the pseudorotation pathway is used as one coordinate, one can obtain the cross-section map in the case of one constant parameter (Fig. 14). For the reason that were discussed for 7-rings, two pseudorotation coordinates — $\psi_2 = 2\psi_3$ and $\psi_2 = 2\psi_3 + 180°$ — also exist for 8-rings, the only difference being that in this case the sign of Θ_m also depends on the sign of q_4. The map presented in Fig. 14 reflects the interrelationship of all conformations for the given cross section. The pseudorotation BC—TBC and the inversion of BC through the LC conformation (or TBC through C) are the most well known. In addition, it is apparent from the map that the previous undescribed $-\frac{-+-}{-+-}+$ and $-\frac{0+-}{0+-}+$

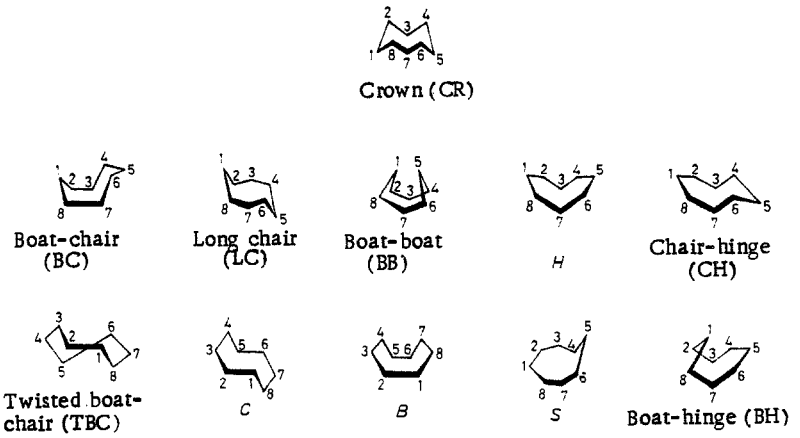

Fig. 13. Some symmetrical conformations of 8-rings.

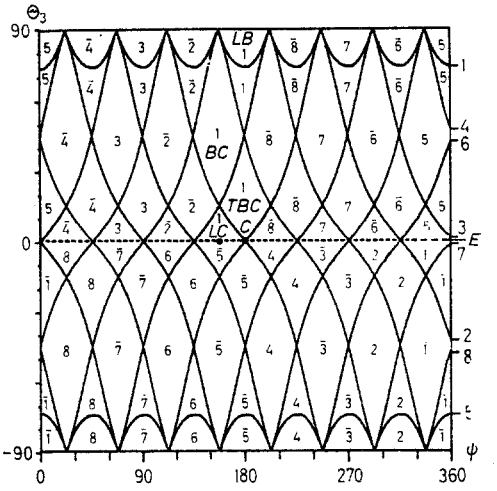

Fig. 14. Cross section of the conformational map of 8-rings with respect to the pseudorotation coordinates ($\psi = \psi_3$ and $\psi = 2\psi_2$ when $\Theta_2 = -45°$).

conformations may also be partners of the pseudorotation of BC.

If $\psi_3 = n\pi/8$ and $\psi_2 = 2\psi_3$ are used as constants, one can obtain cross sections that contain only symmetrical conformations that have a symmetry axis or plane (Figs. 15 and 16). These cross sections encompass virtually all symmetrical conformations of 8-rings. We detected 35 symmetrical conformations, half of which have not been previously described (Tables 5 and 6). Of the total number of conformations, 10 are nonplanar, four are monoplanar, 12 are diplanar, four are triplanar, and five are tetraplanar. In addition, these cross sections reflect all conformational transitions that occur with retention of the symmetry plane or axis. It should be noted that precise values of the FC of the standard conformations are presented only for the highly symmetrical conformations (see Table 4). The FC for the other standard conformations can evidently be determined by calculation of the centers of gravity of the corresponding regions of conformation space.

CONCLUSION

The graphical method of quantitative conformational analysis that we have proposed makes it possible to unambiguously determine the conformations of medium-sized rings and the mode and degree of their distortion. By means of this method one can study and graphically show all possible pathways of conformational interchange and the most probably intermediate conformations without resorting to figures of the individual conformations.

TABLE 4. Highly Symmetrical Conformations of 8-Rings

Conformation*	Folding coordinates				Hendrickson symbol	Symmetry group
	ψ_2	ψ_3	Θ_2	Θ_3		
CR	—	—	90,0	90	$\frac{+-+-}{-+-+}$	D_{4d}
BB	315	—	0,0	90	$\frac{--++}{++--}$	D_{2d}
H	315	—	45,0	90	$\frac{0-+0}{0+-0}$	C_{2v}
LC	—	157,5	90,0	0	$\frac{-++-}{+--+}$	C_{2h}
B	360	—	0,0	90	$-\frac{0+0}{0+0}-$	D_{2d}
LB	360	—	27,4	90	$-\frac{-+-}{-+-}-$	D_2
TH	360	—	54,8	90	$0\frac{-+-}{-+-}0$	D_2
C	—	180,0	90,0	0	$-\frac{+0-}{+0-}+$	C_{2h}

*LB is long boat, and TH is twisted hinge.

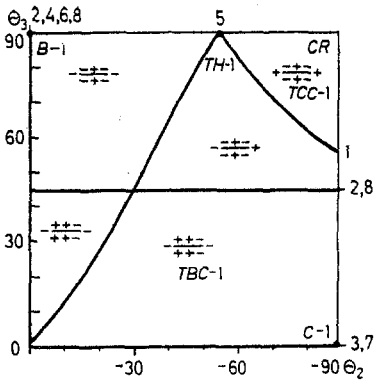

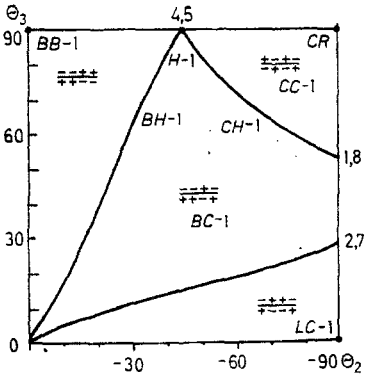

Fig. 15

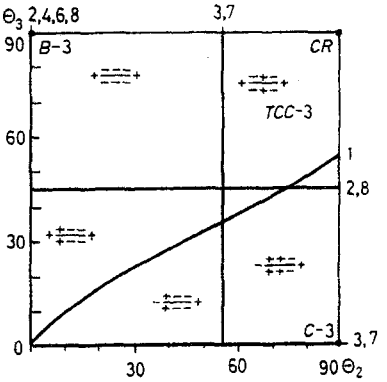

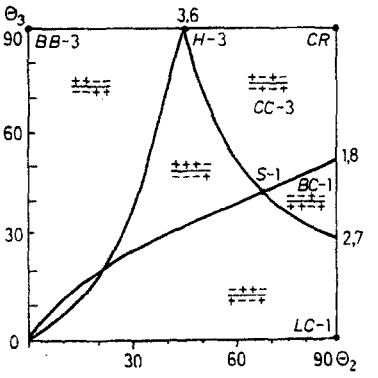

Fig. 16

Fig. 15. Conformational maps of 8-rings for constant ψ_2 = 315° and ψ_3 = 157.5°; the 0-lines are dual; all conformations on these maps have symmetry plane C_s.

Fig. 16. Conformational maps of 8-rings for constant ψ_2 = 360° and ψ_3 = 180°. All conformations on these maps have symmetry axis C_2.

TABLE 5. Approximate Folding Coordinates of Symmetrical Conformations of 8-Rings Having Symmetry Planes C_S (ψ_2 = 315, ψ_3 = 157.5)

Conformation	Θ_2°	Θ_3°	Hendrickson symbol	Conformation	Θ_2°	Θ_3°	Hendrickson symbol
BC	−45	45	$\frac{--+-}{++-+}$	*BB/TC*	22	21	$\frac{0+0-}{0-0+}$
BH	−30	60	$\frac{--+0}{++-0}$	—	45	60	$\frac{+++-}{---+}$
CH	−67	67	$\frac{0-+-}{0+-+}$	—	55	61	$\frac{+0+-}{-0-+}$
BC/TC	−67	21	$\frac{-0+-}{+0-+}$	—	36	55	$\frac{++0-}{--0+}$
S	67	42	$\frac{-+00}{+-00}$	—	45	33	$\frac{0++-}{0--+}$

This method is based on the use of FC. The conformational maps obtained by graphical solution of the equations for the FC of 6-8-rings fix the distribution of all theoretically possible conformations of a given N-ring in the (N − 3)-dimensional space of the FC. This creates a foundation for the rigorous systematization of all standard conformations of medium-sized rings and in a number of cases made it possible to detect previously unknown conformations and pathways of conformational interchange.

TABLE 6. Approximate Folding Coordinates of Symmetrical Conformations of 8-Rings Having Symmetry Axis C_2 ($\psi_2 = 360°$, $\psi_3 = 180°$)

θ_2°	θ_3°	Hendrickson symbol	θ_2°	θ_3°	Hendrickson symbol	θ_2°	θ_3°	Hendrickson symbol
−54	23	$-\frac{++-}{++-}+$*	−15	45	$-\frac{0+-}{0+-}-$	54	40	$+\frac{+0-}{+0-}+$
−30	45	$-\frac{0+-}{0+-}0$**	−10	35	$-\frac{++-}{++-}-$	73	45	$0\frac{0+-}{0+-}+$
−54	45	$-\frac{0+-}{0+-}+$	−22	30	$-\frac{++-}{++-}0$	60	40	$+\frac{++-}{++-}+$
−54	65	$-\frac{-+-}{-+-}+$	30	45	$+\frac{0--}{0--}+$	64	40	$0\frac{++-}{++-}+$
−70	70	$0\frac{-+-}{-+-}+$	54	45	$+\frac{00-}{00-}+$	65	45	$+\frac{0+-}{0+-}+$
−40	65	$-\frac{-+-}{-+-}0$	54	35	$0\frac{+0-}{+0-}+$			

*Twisted boat-chair (TBC).
**B/TBC.

The proposed method opens up a possibility for the systematic investigation of the conformation space also of nine-membered and larger rings, which thus far have been studied only slightly. However, its use is limited by the increase in the complexity of the conformational maps with an increase in the size of the ring. This is a consequence of the increase in the dimensionality of conformation space, which objectively reflects the marked increase in the number of standard conformations and possible pathways of conformational transitions with an increase in N.

For the investigation of the conformations of real molecules by the proposed method one must calculate the FC of a given ring and plot these coordinates on the corresponding map. The principal conformational maps of 6-8-rings are presented in our paper. When the necessary map is not available, it can be obtained by means of the CYCLEK program* or constructed in accordance with the equations presented in this paper. A comparison of the barriers to rotation relative to individual bonds in the ring makes it possible to detect, by means of these maps, the most probable pathways of conformational interchange and the corresponding intermediate conformations. They can also be reproduced on the basis of statistical treatment of the data for a set of related compounds or by using the results of conformational calculations.

LITERATURE CITED

1. J. B. Hendrickson, J. Am. Chem. Soc., 89, 7036 (1967).
2. J. B. Hendrickson, J. Am. Chem. Soc., 89, 7047 (1967).
3. J. E. Kilpatrick, K. S. Pitzer, and R. Spitzer, J. Am. Chem. Soc., 69, 2483 (1947).
4. H. R. Buys and H. J. Geise, Tetrahedron Lett., 5619 (1968).
5. F. H. Cano, C. Foces-Foces, and S. Garcia-Blanco, Tetrahedron, 33, 797 (1977).
6. D. Cremer and J. P. Pople, J. Am. Chem. Soc., 97, 1354 (1975).
7. N. S. Zefirov and V. A. Palyulin, Dokl. Akad. Nauk SSSR, 252, 111 (1980).
8. E. Diez, A. L. Esteban, J. Guilleme, and S. L. Bermejo, J. Mol. Struct., 70, 61 (1981).
9. F. H. Cano, C. Foces-Foces, and S. Garcia-Blanco, Acta Cryst., 34A, 91 (1978).
10. F. H. Cano and C. Foces-Foces, J. Mol. Struct., 94, 209 (1983).
11. E. Diez, A. Esteban, S. L. Bermejo, C. Altona, and F. A. A. M. de Leeuw, J. Mol. Struct., 125, 49 (1984).
12. R. Bucourt, in: Topics in Stereochemistry, Vol. 8, Wiley, New York (1974), p. 159.
13. "International Union of Pure and Applied Chemistry. Reports on symbolism and nomenclature," J. Am. Chem. Soc., 82, 5517 (1960).

*The CYCLEK program for the calculation of the folding coordinates and construction of the conformational maps and cross sections of 6-8-rings is written in FORTRAN-77 and PASCAL languages for the ASPECT-1000 minicomputer of the Bruker WM-360 NMR spectrometer. The program can be sent on request.

14. C. Altona and M. Sundaralingam, Tetrahedron, 26, 925 (1970).
15. R. Bucourt and D. Hainant, Bull. Soc. Chim. France, 4565 (1967).
16. M. D. Walkinshaw, A. H. Cowley, and S. K. Mehrotra, Acta Cryst., 40C, 129 (1984).
17. S. Ariel, J. Trotter, Acta Cryst., 40C, 1253 (1984).
18. J. F. Chiong and S.H. Bauer, J. Am. Chem. Soc., 91, 1898 (1969).
19. H. Koningsveld and J. M. A. Baas, Acta Cryst., 40C, 311 (1984).
20. F. Baert, R. Fouret, M. Sliwa, and H. Sliwa, Tetrahedron, 36, 2765 (1980).
21. E. Miller-Srenger and R. Guglielmetti, Acta Cryst., 40C, 2050 (1984).
22. M. D. Walkinshaw, A. H. Cowley, and S. K. Mehrotra, Acta. Cryst., 40C, 125 (1984).
23. S. S. C. Chu, S. V. L. Narayama, and R. D. Rosenstein, Acta Cryst., 40C, 1281 (1984).
24. D. Bethell, D. Chadwick, G. Q. Maling, and M. M. Harding, Acta Cryst., 40C, 1628 (1984).
25. H. M. Pickett and H. L. Strauss, J. Am. Chem. Soc., 92, 7281 (1970).
26. D. F. Bocian, H. M. Pickett, T. C. Rounds, and H. L. Strauss, J. Am. Chem. Soc., 97, 687 (1975).
27. V. A. Palyulin, N. S. Zefirov, V. E. Shklover, and Yu. T. Struchkov, J. Mol. Struct., 70, 65 (1981).